Surface properties · carbon black · inverse gas chromatography

Very often, authors examine only one carbon black sample of a given type, admitting that the determined characteristics can be extended to all other samples having the same producer specifications. But, due to the variability of the raw materials, that are natural products, and the variability of the process, the surface properties will vary more or less from one batch to another. Nevertheless, the batch to batch stability of filler is of a main importance in the industrial applications. The present work will demonstrate that inverse gas chromatographic methods provide a simple way to test the surface properties of a solid.

Carbon Black using Inverse Gas Chromatography Techniques

Study of the Batch to Batch Stability of the Surface Properties

H. Balard, Mulhouse, E. Brendle, Pulversheim (France)

Einfluss der Batch-Stabilität auf die Oberflächeneigenschaften von Ruß-Verwendung bei der Inversen Gaschromatographie

Oberflächeneigenschaften · Ruß · Inverse Gaschromatographie

Häufig werden einzelne Rußproben einer gewissen Type untersucht und die Ergebnisse auf andere Muster mit der gleichen Spezifikation übertragen. Unterschiede in der Zusammensetzung der Rohstoffe, die natürliche Produkte sind, wie auch die Variabilität der Herstellungsprozesse führt zu Variationen der Oberflächeneigenschaften der jeweiligen Rußproben. Nichtsdestoweniger ist die Konstanz der Qualität von einer gewissen Wichtigkeit für industrielle Anwendungen. Diese Arbeit verdeutlicht, dass die Methode der Inversen Gaschromatographie eine einfache Charakterisierung der Oberflächeneigenschaften darstellt.

Inverse gas chromatography in infinite dilution conditions or at finite concentration conditions had been often used for the characterisation of the surface properties of carbon fibres [1–3], active carbon [4] and carbon blacks [5–10] having different origins or submitted to controlled treatment. Generally, only one carbon black sample of a given type was examined and the results obtained were admitting to be representative of all the carbon samples having the same producer specifications.

But, the variability of the raw materials, which are generally natural products, and the variability of the process will both influence more or less the surface properties from one batch to another. But, the batch to batch stability of filler influences obviously the use properties of the finished products and is therefore of a main importance in the industrial applications.

Hence the surface properties of 12 carbon black N550 samples corresponding to twelve different batches, were examined in order to demonstrate that inverse gas chromatographic analytical methods provide a good way to test their surface property stability from one batch to another one.

Experimental part

Samples

Twelve rubber reinforcing carbon black samples N550 from (Columbian Carbon USA) were selected having both a specific surface area of about 50 m^2g, but coming from different manufacturing batches.

Inverse Gas Chromatography (IGC)

IGC may be performed either at the infinite dilution conditions (IGC-ID), but also at finite concentration conditions (IGC-FC). In the first instance, the measured quantity is the net retention time (t_r), i. e., the time the injected solute spends inside the GC column, corrected by the time it would take for it to cross the column without adsorption on the chromatographic support. This latter time is measured using a solute that scarcely adsorbs under the given experimental conditions (methane). From t_r, one easily computes the net retention volume V_n knowing the flow rate of the carrier gas. It seems obvious that the "affinity" of the solid support inside the column (the carbon sample) will directly influence V_n. When measured under equilibrium conditions, V_n leads to the standard variation of the free energy of adsorption of the solutes.

In the finite concentration mode, measurable amounts of solutes are injected leading to deformed chromatographic peaks. From the peak deformation, adsorption isotherms and adsorption energies distribution are calculated.

Sample preparation

Experimentally, the carbon samples were sieved to select the fraction of particles having diameters between 250 and 400 µm. Then, the selected particles

were introduced in a stainless GC steel column. A commercial gas chromatographic apparatus (Intersmat, model IGC 120 DFL), equipped with a highly sensitive flame ionization detector, was used for this study. Helium was selected as carrier gas at a flow of 25 ml/min. The IGC-ID measurements were performed at 110 °C and the IGC-FC ones, at 50 °C.

Theoretical part

IGC-ID

In IGC-ID approach, a very minute amount of probe corresponding to the detection threshold of a FID detector is injected and the net retention volume of the probe is recorded, which is the experimental data, reflecting the level of interaction between the solid surface and the probe.

On *Figure 1*, the free energy of some IGC probes having different nature – apolar, n-alkanes, polar or sterically hindered, cyclic or branched alkanes- are plotted versus their Brendlé and Papirer index of morphology X_t, a parameter closely related to the molecular polarisabilty of the probes.

This figure describes the principle of the determination of main thermodynamical parameters, which can be acquire trough IGC-ID technique and related respectively:

– the increment of free energy per methylene group ($\delta\Delta G_a^{CH2}$), which is equal to the slope of the n-alkane straight line and related to the non-specific potential of interaction of the surface through London's forces,
– the increment of free energy to its specific capacity of interaction ($\delta\Delta G_a^{sp}$) which is given by the vertical departure of the representative point of a given polar probe from n-alkane straight line,
– the decrement of free energy ($\delta\Delta G_a^{M}$), defined as the departure of the representative point of a cyclic or a branched alkane from the n-alkane straight line and related to the size exclusion effect that can takes place when the studied solid surface exhibits a surface roughness at a molecular level.

The principle of the calculation of the main CGI-DI values – γ_s^d, I_M and are recalled thereafter.

Dispersive component of the surface energy

Using IGC-ID, the dispersive component of the surface energy was determined calling on the Doris and Gray approach [12] by injecting a set of linear alkane in the column field with solid of interest. When plotting the free ad sorption energy versus their topological indices (here, their number of carbon atoms) one obtains the "alkane line" which the slope corresponds to the increment of free energy per methylene groups ($\delta\Delta G_a^{CH2}$).

Applying the previous approach, the dispersive component of the surface energy (γ_s^d) can be readily calculated according to the equation (1).

$$\gamma_s^d = \frac{(\delta\Delta G_a^{CH2})^2}{4N^2 a_{CH_2}\gamma_{CH_2}} \qquad (1)$$

where N is Avogadro's number, a_{CH2} is the area covered by one methylene group (0.06 nm^2), and γ_{CH2} is the surface energy of pure methylene group surface, i. e., polyethylene, $\gamma_{CH2} = 35.6 + 0.058\,(293 - T)$, in mJ/m^2, whereas ΔG_{CH2} is obtained from the slope of the straight line obtained when plotting the $\delta\Delta G$ of n-alkane probes versus their topological indices or their number of carbon atoms, namely (2):

$$\delta\Delta G_{CH2} = -RT \ln \frac{V_{n_{(n)}}}{V_{n_{(n+l)}}} \qquad (2)$$

γ_s^d is directly related to the surface polarisability of the solid surface.

Index of nano-morphology

Of course, probes other than the linear apolar n-alkanes may be used to assess the interaction potential of a solid surface. Among these probes, branched or cyclic isomers of the n-alkanes that can only exchange non-specific interaction as the linear isomers, are of a main interest for testing the surface morphology at a molecular scale. In particular, Balard and Papirer [13] have shown that such isomers exhibit much lower retention times than the corresponding linear alkanes for solids having a lamellar structure such as crystalline silicas or talc, thus demonstrating that the assumption of surface flatness is not fulfilled.

When stereochemistry hinders branched or cyclic isomers from entering structures in which linear alkanes could absorb, much lower retention times are observed for non-linear isomers than for the linear ones. Nevertheless, on a flat surface on which no size exclusion effects take place, linear and branched or cyclic alkanes behave differently, due to their difference of polarisabilty. In order to take into account this last parameter, Brendle and Papirer [11] had proposed the topology indices X_t, adapted to IGC-ID measurements, derived from Wiener's topology indices.

Size exclusion effect leads to a decrease of the free energy of adsorption when comparing with that of a virtual linear alkane having the same topological index (X_t). The departure of the representative point of the branched or cyclic alkane from the n-alkane line gives a measure of the size exclusion effect. Balard et al [14] have proposed the indices of surface nano-morphology, according to the equation (3):

$$I_M = \exp\left(\frac{-\Delta G_a^M}{R.T}\right) \qquad (3)$$

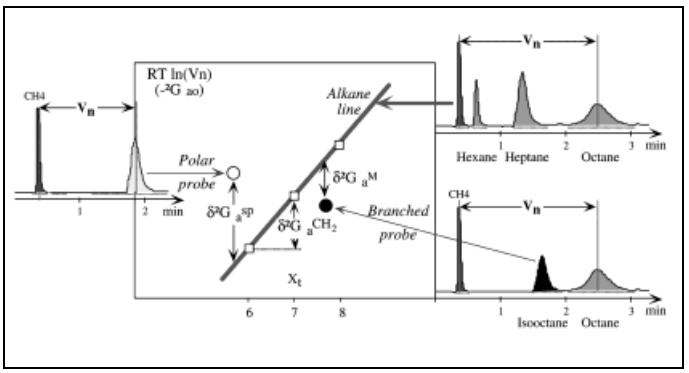

Figure 1. Variation of the free energies of adsorption of the probe with their topological indexes: relation with some experimental chromatograms and principle of the determination of main IGC-ID parameters, $\delta\Delta G_a^{CH2}$, $\delta\Delta G_a^{sp}$ and $\delta\Delta G_a^{M}$.

When I_M is equal to 1, the solid surface can be considered as flat at the molecular level. As the surface roughness increases decreases readily down to a value of 0.1 for some solids like talcs [15] or clays [16].

Specific component of the surface energy

Specific interactions include all types of interactions except the London or dispersive interactions. Among them, acid-base interactions play a determinant role [14]. As pointed out above, a comparison of the apolar (n-alkanes) and polar probe adsorption behaviours leads to the evaluation of the contribution of the specific interactions ($\delta\Delta G_a^{sp}$), by subtracting, from the global free energy variation ΔG_a, the contribution due to dispersive interactions. The latter is estimated from the "n-alkanes reference line" observed when plotting the global free energy of adsorption ΔG_a of n-alkanes versus their topological indices. The contribution of specific interactions ($\delta\Delta G_a^{sp}$) is then given by the departure of the representative point of the polar probe from this "reference alkane line" as shown on Figure 1. The representative points of a polar probe, that is more interactive with a polar surface, should be located above the "linear alkane line".

Limitations of IGC-ID

It is of importance to realise that IGC-ID delivers absolute thermodynamic parameters only on a perfectly homogeneous surface. No real solid surface could be considered as truly homogeneous and obviously, the presence of sites having different potentials of interaction necessarily influences the IGC-ID behaviour of the probe through a strong variation of the residence time on the different visited adsorption sites. Then, the overall retention time is a complex function of the number of sites, their characteristic energies of interaction and their capture radius. Consequently, the thermodynamic data delivered by the IGC-ID can only be used for the comparison of solid surfaces presenting a close analogous surface structure.

IGC-FC

On the contrary to the IGC-ID, a finite volume of liquid probe is injected into the chromatographic device, here the injected volume could be equal up to about 20 µl depending of adsorption surface area of the solid contained in the column. IGC-FC gives access to adsorption isotherms [17]. The simplest method, from the point of view of the analysis duration, is "the elution characteristic point method" (ECP) that allows the acquisition of part of the desorption isotherm from a unique chromatographic peak.

Using this method, the first derivative of the adsorption isotherm can be readily calculated starting from the retention times and the signal heights of characteristic points taken on the diffuse descending front of the chromatogram, according to equation (4):

$$\left(\frac{\partial N}{\partial P}\right) = \frac{JDt'}{mRT} \qquad (4)$$

where, N is the number of absorbed molecules, P the pressure of the probe at the output of the column, t_r' the net retention time of a characteristic point on the rear diffuse profile of the chromatogram, J the James and Martin's coefficient (xx JM), D the output flow rate and m the mass of adsorbent.

According to ECP approach [17], the isotherm of desorption can be readily calculated. Several information may be extracted from the isotherms: BET specific surface area, BET and Henry's constants as depicted on *Figure 2*. Moreover, it is obvious that the shape of the desorption isotherm depends on the surface heterogeneity.

Intuitively, molecules adsorbed on the sites having the highest energy will remain a longer time in the chromatographic column than those they have visited sites having a lower energy. Hence, the shape analysis of the isotherm will give access to the distribution function of the adsorption energies that looks like that represented on the right part of the Figure 2.

For the shape analysis of the desorption isotherm, a physical model is required. Generally, one admits that the global isotherm can be considered as a sum of local isotherms of adsorption on isoenergetic domains [18]. Then, the surface heterogeneity is described by a distribution function corresponding to the relative abundance of each type of domain having the same characteristic energy of interaction (ε). This characteristic energy is related to the pressure of measurement [19] by equation (5):

$$E = C \times 10^4\ (MT)^{1/2} \qquad (5)$$

where M is the probe molecular weight and T is the experimental temperature (K) and C a constant depending of the pressure unit: $C = 2.346\ 10^3$ when the pressure is expressed in kPa.

Taking into account the previous physical model, the general equation, which describes the physical adsorption on heterogeneous solid surface, is usually written in the following integral form (6):

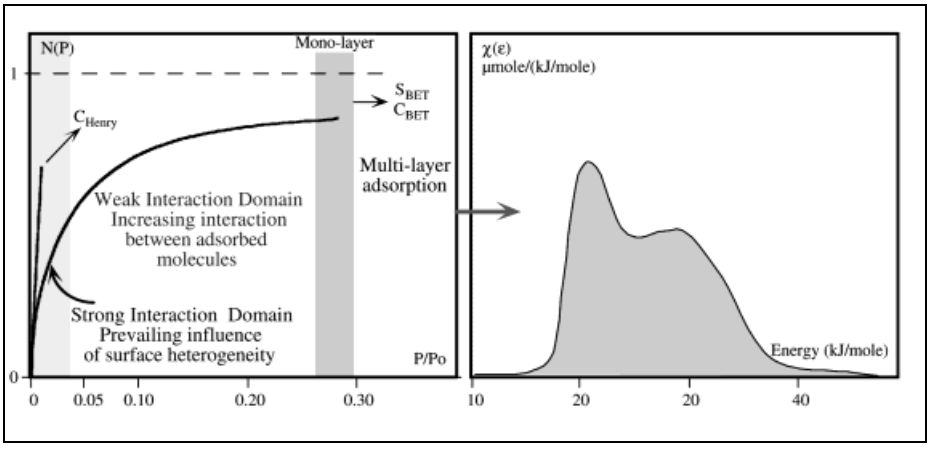

Figure 2. Relation between the isotherm of desorption and the surface heterogeneity and a typical distribution function of the energies that can be observed of an alcohol probe on a silica sample.

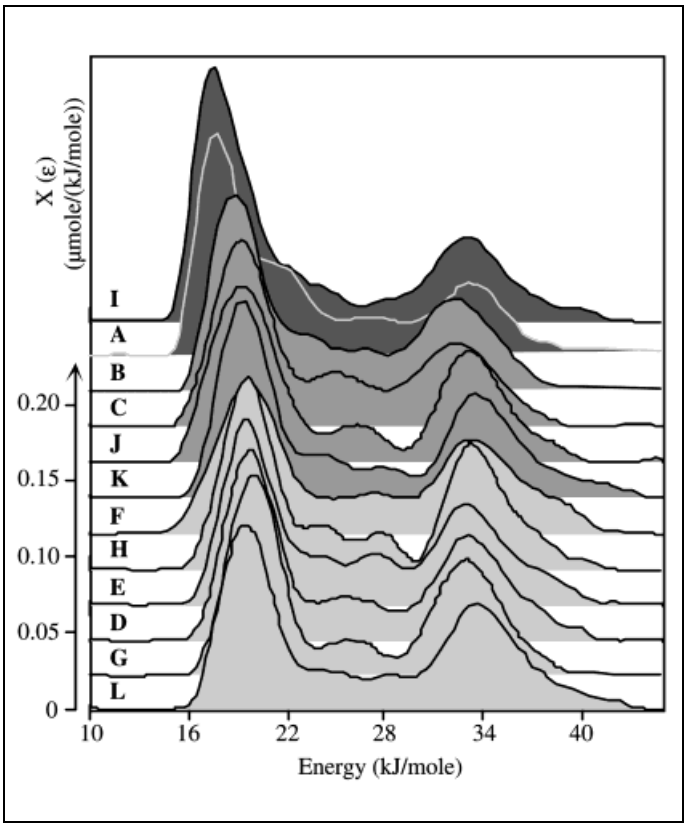

Figure 3. Variation of the nano-morphological indexes with the dispersive component of the surface energy.

$$N(T,\ P) = N_0 \int_{\Omega} \theta(\varepsilon,\ T,\ P)\ \chi(\varepsilon)d\varepsilon \quad (6)$$

where N(T,P) is the number of molecules adsorbed at the pressure p and at the temperature T of measurement, N_0 is the number of molecules corresponding to the formation of a monolayer, $\theta(\varepsilon,\ T,\ P)$ is the local isotherm (generally the Frumkin, Fowler, Guggenheim's isotherm) corresponding to adsorption sites having the same characteristic adsorption energy ε, $\chi(\varepsilon)$ is the so-called adsorption energy distribution function (DF) describing the energies which exist at the gas-solid interface and Ω is the physical domain of the adsorption energy.

From a mathematical point of view, solving the former integral equation is not a trivial task because it has no general solution, except when one adopts a step function as local isotherm that says the condensation approximation. The condensation approximation supposes that the sites of adsorption of given energy are unoccupied below a characteristic pressure and entirely occupied above it. The distribution function for the condensation approximation (DFCA) is directly related to the first derivative of the isotherm corrected for the multilayer adsorption, according to equation 7:

$$\chi_{CA}(\varepsilon) = \frac{P'}{RT}\ \frac{\partial}{\partial P'}\ \left[\frac{N'(P')}{N_0}\right] \quad (7)$$

where: N' and P' are respectively the amount of adsorbed probe and the equilibrium pressure of the probe corrected for the multilayer adsorption, N_0 is the amount of adsorbat corresponding to the monolayer formation, R the universal gas constant for an ideal gas and T the absolute temperature at which the measurement is performed.

The first derivative of the isotherm corrected for the multi-layer adsorption [9] (experimental isotherm of type II) is related to the experimental isotherm and its first derivative by the following equation 8:

$$\frac{\partial N'}{\partial p'} = (1-x)^3\ \frac{\partial N}{\partial p} - (1-x)1^2\ \frac{N}{P_0} \quad (8)$$

The condensation approximation is all the better as the temperature of measurement approaches the absolute zero. In the usual IGC measurements conditions, at room temperature and above room temperature, this approximation fails completely and it becomes necessary to use other approximated forms of the local isotherm. Among them, for Langmuir local isotherms, the extended Rudzinski et al method [20] allows the computation of the actual distribution function (DFRJ) from a limited development of the even derivatives of the DFCA, according to equation (9):

$$\chi(\varepsilon) = \overset{+}{}_{j=0}\ (RT)^{2j} b_{2j} \cdot \dot{\chi}_{CA}^{(2j)}(E)$$

$$(\varepsilon \text{ with } b_0 = 1 \text{ and } b_{2j} = (-1)^j\ \frac{\check{s}^{2j}}{(2j+1)!} \quad (9)$$

The use of a signal treatment method, based on Fourier's transforms, allows the filtration of the isotherm data (elimination of the experimental noise contribution). The remarkable robustness of this new approach, versus noise and irregular sampling, was carefully tested and the energetic surface heterogeneity of a series of solids [21–25] was evaluated.

Results

IGC-ID analysis

Dispersive and specific interaction capacities and surface nano-morphology.

Injecting branched or cyclic alkane probes, calling on size exclusion IGC [14], the surface nano-morphology of the carbon blacks was assessed. Lower the nano-morphological index (I_M) is low, higher the surface roughness is.

On another hand, polar probes, which can exchange only specific interactions with the carbon black surface, like chloroform or benzene, were also injected in order assess the capacity of specific interaction of the carbon black samples.

The measured values of γ_S^D, I_M and I_{SP} are gathered in the *Table 1*.

On the point of view of IGC-ID, strong variations of the surface properties of these samples are evidenced, e. g. the γ_S^D values vary from 170 mJ/m^2 to 353 mJ/m^2. As previously observed on other solids [13] a correlation was observed between the γ_S^D values and the index of morphology as depicted on *Figure 3*, for Hexamethylethane or cyclooctane probes.

Table 1. IGC-ID main characteristics of the studied carbon black samples.

Carbon	γ_S^D	$-I_M$ (DMH)	$-I_M$ (HME)	$-I_M$ (C-C8)	I_{sp} ($CHCl_3$)	I_sp (Bz)
A	208	0,62	0,71	0,29	5,8	3,89
B	211	0,62	0,63	0,27	8,78	3,29
C	**252**	**0,28**	**0,42**	**0,13**	**9,03**	**high**
D	210	0,68	0,6	0,28	8,42	3,79
E	**353**	**0,5**	**0,28**	**0,09**	**10,06**	**3,54**
F	180	0,69	0,71	0,34	7,62	3,35
G	188	0,54	0,66	0,31	8,08	3,64
H	*170*	*0,71*	*0,66*	*0,34*	*7,33*	*3,71*
I	**289**	**0,63**	0,55	0,24	**9,7**	**6,38**
J	197	0,61	0,57	0,29	8,53	3,99
K	192	0,65	0,6	0,31	8,51	4,11
L	*174*	*0,71*	*0,64*	*0,35*	*8,18*	*4,57*

Bold characters indicates IGC characteristics that stay clearly above the mean values, whereas *italic* ones are related to the most lower values comparing to mean ones.

Table 2. IGC-FC main characteristics of the studied carbon black samples.

Sample ref.	S_{SPE} (m^2/g)	C_{BET}
A	54	*14*
B	51	19
C	**74**	19
D	51	**27**
E	49	**27**
F	50	26
G	*47*	**27**
H	49	26
I	**83**	*10*
J	56	20
K	51	23
L	49	**28**

Bold characters indicates IGC characteristics that stay clearly above the mean values, whereas *italic* ones are related to the most lower values comparing to mean ones.

Hence, higher dispersive surface energies correspond to higher surface roughness on the probe size level. This phenomena is certainly related to the presence of fish scale like structures according to the Donnet's model in which the linear alkane probes may insert and from which bulky alkane probes are excluded.

Finally, it is also obvious that 3 samples (C, E and I) exhibit clearly very different IGC-ID characteristics and a close examination of the specific parameter of chloroform and benzene probes confirms this observation.

Because IGC-ID is mainly sensitive to the sites having the highest energy, the values measured on an heterogeneous solid have no absolute signification and are only apparent values. Hence, the IGC-CF was called on in order to assess their surface heterogeneity.

IGC-FC analysis

Specific surface area and BET constant

Hence, the surface properties of these twelve samples were examined using IGC-FC and their specific surface areas and BET constants were computed from the hexane isotherm of desorption. Their values measured on the twelve samples are reported in the *Table 2*.

As previously for IGC-ID data, the sample (I) exhibits very different IGC-FC characteristics: a high specific area and a low BET constant value. To some extent, sample C is also out of range on the point of view of its specific surface area. The BET specific surface area measured for the other samples are equal to the attempted values for N550 carbon blacks.

It is also worth to point out that the BET constants vary in large extend from 10 to 28, emphasising a strong variation of the potential of interaction of these fillers at high coverage ratios. Finally the distribution were computed according to Rudzinski-Jagiello approach and using our calculation method [20]. They are shown on *Figure 4*, sorted by increasing BET constants, from top to bottom.

If all the distribution functions present an analogous shape with a main peak centred on 18 kJ/mole and another one centred at 32–34 kJ/mole. If the position of the latter peaks is quite stable, a continuous shift of the position of the former peaks is observed toward the low energies, whereas their relative intensity increase, with decreasing BET constants.

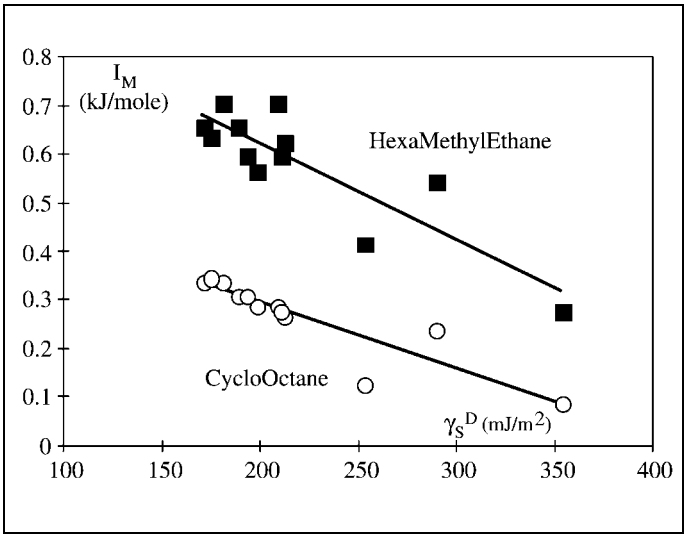

Figure 4. Distribution function of the energies of adsorption of hexane probe, on studied N550 carbon black samples, measured at 50 °C.

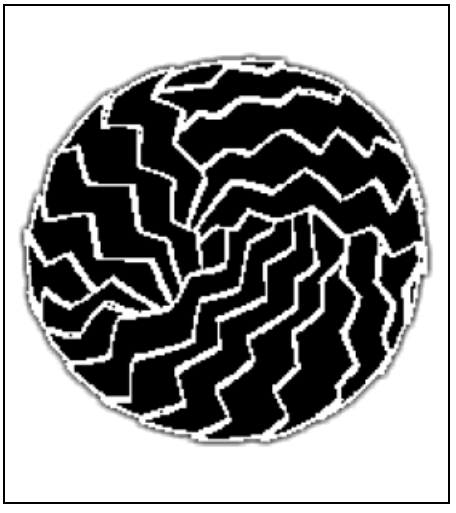

Figure 5. Donnet's model of carbon black.

Correlatively, the intensity of the intermediate part of the distribution increases and its shape follows a continuous evolution. From their aspects, they could be roughly classified in 3 groups depicted on Figure 4, according to the grey scale. The sample I and in a less extend the sample A exhibit very different distribution function shape.

A tentative interpretation of these distribution functions could be done, based on a study led on graphite, fullerene and other carbon black samples [9]. The peak situated at low energy could be attributed to the graphitic domains present on the carbon black surface, revealed by STM microscopy and schematised to the Donnet's model [26] depicted on *Figure 5*. The other main peaks at high energy would be related to the "lateral surfaces" of these graphitic domains and is also observed in case of graphite samples. The intermediate part would be characteristic of the amorphous part of the surface which will certainly contain the most part of the functionnal groups. Hence, IGC analysis highlights that the graphitic character of the studied samples varies in a relative large range due to the variability of the process.

Conclusion

If, very often, authors examine only one carbon black sample of a given type, admitting that the determined characteristics can be extended to all other samples having the same producer specifications. The present work demonstrates that this assumption is not generally full filled and that due to the variability of the raw materials and/or of the process, the surface properties will vary more or less from one batch to another. Then, considering that the batch to batch stability of filler is of a main importance in the industrial applications, the present work demonstrates that inverse gas chromatographic methods provide a simple and powerful way to test finely to the surface properties of a solid.

References

[1] S.J. Park and J.B.Donnet, Carbon **29** (1991) 955.
[2] A. Quinn and J.B. Donnet, Carbon **32** (1994) 165.
[3] A. Van-Asten, N. Van-Veenendaal and S. Koster, J. Chromatogr **888** (2000) 175.
[4] R. Leboda, Materials Chemistry and Physics **31** (1992) 243.
[5] C. Lansinger and J.B. Donnet, Kautschuk. Gummi Kunstst. **45** (1992) 459.
[6] W.D. Wang, A. Vidal, M.J. Wang and J.B. Donnet, Kautschuk Gummi Kunstst. **46** (1993) 770.
[7] W.D. Wang, B. Haidar, A. Vidal and J.B. Donnet , Kautschuk. Gummi Kunstst. **47** (1994) 238.
[8] W.D. Wang, A. Vidal, G. Nanse and J.B. Donnet, Kautschuk, Gummi, Kunstst. **47**(1994) 493.
[9] E. Papirer, E. Brendlé, H. Balard and F. Ozil, Carbon **37** (1997) 1265.
[10] H. Darmstadt , N.Z. Cao, D.M. Pantea, C. Roy, L. Summchen, U. Roland , J.B. Donnet, T.K. Wang, C.H. Peng and P.J. Donnelly, Rubber Chem. Technol. **73** (2000) 293.
[11] E. Brendle and E. Papirer, J. Colloid Interf. Sci. **194** (1997) 217.
[12] G.M. Dorris and D.G. Gray, J.Colloid Interf. Sci. **71** (1979) 97.
[13] E. Papirer and H. Balard, Studies in Surface Science and Catalysis, ed. Dabrowski A. and Tertykh V.A., Elsevier, Amsterdam **99** (1995) 479.
[14] H. Balard, E. Brendlé and E. Papirer, Acid-Base Interactions: Relevance to Adhesion Science and Technology, K. Mittal ed., VSP, Utrecht (Nederlands) (2000) 14.
[15] M.P. Comard, R. Calvet, S. Del-Confetto, J. Dodds and H. Balard, Macromol. Symp. Macromolecular Symposium **169** (2001) 19.
[16] A. Saada, B. Siffert, H. Balard and E. Papirer, J. Colloids and Interf. Sci. **175** (1995) 212.
[17] J.R. Conder and C.L. Young, Physicochemical Measurements by Gas Chromatography, Wiley, New York, (1979).
[18] W. Rudzinski and J. Jagiello, J.Colloid Interf. Sci. **87** (1982) 478.
[19] J.P. Hobson, Canad.J. Physics **43** (1965) 1941.
[20] H. Balard, Langmuir **13** (1997) 1260.
[21] H. Balard, A. Saada, J. Hartmann, O. Aouadj and E. Papirer, Makromol. Chem, Makromol. Symp. **108** (1996) 63.
[22] H. Balard, O. Aouadj and E. Papirer, Langmuir **13** (1997) 1251.
[23] H. Balard, A. Saada, E. Papirer and B. Siffert, Langmuir **13** (1997) 1256.
[24] H. Balard, E. Papirer, A. Khalfi, H. Barthel and J. Weis, Organosilicon IV: From molecules to materials, Eds. N. Auner and J. Weis, J.Wiley, Weinheim Germany (2000) p 773–792.
[25] E. Papirer, E. Brendlé, H. Balard and F. Ozil, Carbon **37** (1999) 1265.
[26] J.B. Donnet and E. Custodéro , Carbon **30** (1992) 813.

Corresponding author
Eric Brendle
IGC Lab SaRL
Careau Rodolphe
Route de Gebwiller
68840 Pulversheim/Frankreich